
Article:
Shen, Q., Liu, W., Cui, W. et al. (3 more authors) (2015) Low-Complexity Direction-of-Arrival Estimation Based on Wideband Co-Prime Arrays. IEEE/ACM Transactions on Audio, Speech and Language Processing, 23 (9). 1445 - 1456. ISSN 2329-9290

https://doi.org/10.1109/TASLP.2015.2436214

Low-Complexity Direction-of-Arrival Estimation Based on Wideband Co-Prime Arrays

Qing Shen, Wei Liu, *Senior Member, IEEE,* Wei Cui, Siliang Wu, Yimin D. Zhang, *Senior Member, IEEE,* and Moeness G. Amin, *Fellow, IEEE*

***Abstract*—A class of low-complexity compressive sensing based direction-of-arrival (DOA) estimation methods for wideband co-prime arrays is proposed. It is based on a recently proposed narrowband estimation method, where a virtual array model is generated by directly vectorizing the covariance matrix and then using a sparse signal recovery method to obtain the estimation result. As there are a large number of redundant entries in both the auto-correlation and cross-correlation matrices of the two sub-arrays, they can be combined together to form a model with a significantly reduced dimension, thereby leading to a solution with much lower computational complexity without sacrificing performance. A further reduction in complexity is achieved by removing noise power estimation from the formulation. Then, the two proposed low-complexity methods are extended to the wideband realm utilizing a group sparsity based signal reconstruction method. A particular advantage of group sparsity is that it allows a much larger unit inter-element spacing than the standard co-prime array and therefore leads to further improved performance.**

***Index Terms*—Microphone arrays, direction-of-arrival estimation, sparsity, wideband, co-prime.**

I. Introduction

Traditionally, for wideband uniform linear arrays (ULAs), including microphone arrays, the minimum inter-element spacing between adjacent sensors is less than $\lambda_{\min}/2$ to avoid spatial aliasing, where $\lambda_{\min}$ is the minimum wavelength within the frequency band of interest [3]–[5]. This can be problematic when considering arrays with a large aperture size, due to the cost associated with the number of sensors. In the past, sparse arrays have been proposed as a solution [6]–[12], where their non-uniform configuration can avoid grating lobes, while allowing adjacent physical sensor spacings to be greater than $\lambda_{\min}/2$.

Recently, a new class of sparse arrays, referred to as co-prime arrays, was proposed [13], [14]. Assume M and N are co-prime. Then, a co-prime array can be constructed by two sub-arrays, with number of sensors varying based on the values of M and N. A typical co-prime array consists of two sub-arrays sharing a sensor at the zeroth position, one with $2M$ sensors and the other with N sensors. The adjacent sensor spacing for the first sub-array is Nd, while it is Md for the second sub-array, where d is the unit inter-element spacing and also the adjacent virtual sensor spacing of the resultant co-prime difference array (as a result, we need to have $d \leq \lambda/2$, where λ is the operating frequency of the co-prime array). As such, with a total number of $2M + N - 1$ sensors, the difference co-array of the two sub-arrays can provide more than MN degrees of freedom. The increased degrees of freedom (DOFs) can be exploited for effective direction of arrival (DOA) estimations [14]–[17]. In [14], a virtual array of a larger aperture is generated from the co-prime array by vectorizing the covariance matrix, with equivalent coherent impinging signals. Then, a rank restoring method based upon spatial smoothing is utilized for DOA estimation [18], [19]. Under the condition of imperfect correlation matrix, sparsity-based signal recovery method is applied in [15]. In [17], a sparse signal recovery method based on compressive sensing is used for narrowband DOA estimation, employing a ULA with two co-prime frequencies. The aforementioned methods were all designed for narrowband waveforms.

For wideband DOA estimation, several methods have been proposed, most notably the incoherent signal subspace method [20], the coherent signal subspace method [21], the test of orthogonality of projected subspaces method [22], and the recently proposed approximate maximum likelihood approach [23]. In particular, a series of DOA estimation methods based on the sparse signal recovery approach were developed in [24], [25]. In [26], a subband information fusion method based on the concept of group sparsity is introduced to jointly explore the information in all subbands.

Most recently, we have extended the work in [16] to wideband DOA estimations using sparse reconstruction and group sparsity techniques [1]. In essence, the wideband signals received by the array are decomposed into different frequencies/subbands by a discrete Fourier transform (DFT) or, more generally, a filter bank system. Virtual arrays are then formed by vectorizing the covariance matrix in each subband. In this case, the equivalent signal vector of each virtual array is a column vector consisting of all impinging signal powers. In order to jointly exploit the information provided by all subbands, the group-sparsity based signal reconstruction method is employed for enhanced wideband DOA estimation.

However, one problem associated with the above method is its extremely high computational complexity. We recognize that the virtual array model proposed in the narrowband case in [16] includes a large number of redundant entries in both the auto-correlation and the cross-correlation matrices [2]. These redundancies can be combined to form a model with a significantly reduced dimension, thereby leading to a solution with a lower computational complexity without sacrificing performance. A further reduction of complexity is achieved by considering that the estimation result for noise power can be removed from the problem formulation. These newly derived low-complexity methods are then extended to the wideband case by employing the group-sparsity based signal reconstruction method to jointly exploit the information

The work of Y. D. Zhang and M. G. Amin was supported in part by the Office of Naval Research under Grant N00014-13-1-0061. Part of the work was published in [1] and [2].

Q. Shen is with the School of Information and Electronics, Beijing Institute of Technology, Beijing, 100081, China, and also with the Department of Electronic and Electrical Engineering, University of Sheffield, Sheffield, S1 3JD, UK (e-mail: q.shen@sheffield.ac.uk).

W. Liu is with the Department of Electronic and Electrical Engineering, University of Sheffield, Sheffield, S1 3JD, UK (e-mail: w.liu@sheffield.ac.uk).

W. Cui and S. Wu are both with the School of Information and Electronics, Beijing Institute of Technology, Beijing, 100081, China (e-mail: {cuiwei,siliangw}@bit.edu.cn).

Y. D. Zhang and M. G. Amin are both with the Center for Advanced Communications, Villanova University, Villanova, PA 19085, USA (e-mail: {yimin.zhang,moeness.amin}@villanova.edu).

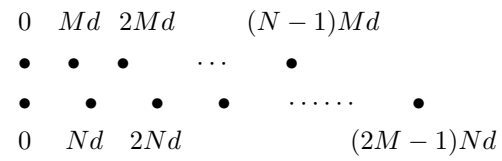

Fig. 1. Structure of a general co-prime array.

provided by all subbands. It is shown that, with a much lower computational complexity, the proposed methods for the single frequency case achieve a very similar performance to the existing one, whereas their respective wideband extensions exhibit a significantly improved performance compared to the narrowband ones.

It is well-known that the resolution of an array improves with an increased aperture size. However, to avoid aliasing, traditionally, a spacing between adjacent sensors of a ULA smaller than $\lambda_{\min}/2$ is commonly used. An advantage of the proposed group sparsity based methods is that the equivalent spacing d between adjacent virtual sensors of the co-prime array can be increased beyond $\lambda_{\min}/2$, while still avoiding spatial aliasing in the estimated results. This is because aliasing locations for different frequencies are different and our group sparsity based methods will force a common sparsity location across all frequencies, corresponding to the true location of the impinging signals. In this respect, we enable the use of a larger inter-element spacing than that associated with the standard co-prime array, leading to a further improved DOA estimation performance.

Our contributions are therefore: 1) Developing the group sparsity-based wideband DOA estimation beyond our preliminary results in [1]; 2) Developing low complexity narrowand and wideband DOA estimation using sparse reconstruction by removing the noise term and recognizing the built in redundancies in subarray auto-correlation and cross-correlation lags; 3) Extending the array aperture by permitting a larger sensor spacing than that defined by half of the minimum wavelength.

This paper is organized as follows. The wideband signal model for co-prime arrays is presented in Section II. The proposed low-complexity DOA estimation method is introduced in Section III for a single frequency. Their wideband extensions are then given in Section IV-A to Section IV-C, and the co-prime arrays with further improved performance due to an increased spacing is presented in Section IV-D. Simulation results are provided in Section V, and results based on collected acoustic data is presented in Section VI. Conclusions are drawn in Section VII.

II. Signal Model with Co-Prime Arrays

A co-prime array consists of two uniform linear sub-arrays, as shown in Fig. 1, where $M < N$ is assumed. The first sub-array has N sensors with an inter-element spacing of Md, and the second one has $2M$ sensors separated by Nd, where $d \leq \lambda_{\min}/2$. Note another layout of the co-prime array uses M sensors for the second sub-array, instead of $2M$. The proposed methods here are equally applicable to both cases.

The zeroth positions of the two sub-arrays share the same sensor and in total there are $2M + N - 1$ sensors. Denote the set of sensor positions for the two sub-arrays as S_1 and S_2, respectively. The zeroth sensor is removed in S_2 for convenience of formulation at a later stage, i.e.,

$$\begin{aligned} S_1 &= \{Mnd,\ 0 \leq n \leq N-1, n \in \mathbf{Z}\}\ , \\ S_2 &= \{Nmd,\ 1 \leq m \leq 2M-1, m \in \mathbf{Z}\}\ , \end{aligned} \tag{1}$$

where $\mathbf{Z}$ is the set of all integers.

Assume that there are K uncorrelated wideband signals $s_k(t)$ with the same bandwidth impinging from incident angles $\theta_k,\ k = 1, 2, \ldots, K$, respectively, where θ_k is measured from the broadside of the array. Then, the signals observed from an element in the two sub-arrays can be expressed as:

$$\begin{aligned} x_{1,n}(t) &= \sum_{k=1}^{K} s_k\left[t - \tau_{1,n}(\theta_k)\right] + \overline{n}_{1,n}(t)\ , \\ x_{2,m}(t) &= \sum_{k=1}^{K} s_k\left[t - \tau_{2,m}(\theta_k)\right] + \overline{n}_{2,m}(t)\ , \end{aligned} \tag{2}$$

where $0 \leq n \leq N-1$ and $1 \leq m \leq 2M-1$. Take the zeroth position of the co-prime array as the reference. Then, $\tau_{1,n}(\theta_k)$ and $\tau_{2,m}(\theta_k)$ represent the time delay of the k-th impinging signal with the incident angle θ_k arriving at the n-th sensor of the first sub-array and the m-th sensor of the second sub-array, respectively. $\overline{n}_{1,n}(t)$ and $\overline{n}_{2,m}(t)$ are white noise at the corresponding sensors.With a sampling frequency f_s, the discrete version of the two sets of sub-array signals can be expressed as

$$\begin{aligned} \mathbf{x}_1[i] &= \left[x_{1,0}[i], x_{1,1}[i], \ldots, x_{1,N-1}[i]\right]^T\ , \\ \mathbf{x}_2[i] &= \left[x_{2,1}[i], x_{2,2}[i], \ldots, x_{2,2M-1}[i]\right]^T\ , \end{aligned} \tag{3}$$

where $\{\cdot\}^T$ denotes the transpose operation and i the discrete-time variable.

Each received sensor signal is divided into non-overlapping groups with length L, and an L-point DFT is applied. Then, the l-th frequency bin/subband samples of the p-th group for each sub-array can be grouped into one vector as follows

$$\begin{aligned} \mathbf{X}_1[l,p] &= \left[X_{1,0}[l,p], X_{1,1}[l,p], \ldots, X_{1,N-1}[l,p]\right]^T\ , \\ \mathbf{X}_2[l,p] &= \left[X_{2,1}[l,p], X_{2,2}[l,p], \ldots, X_{2,2M-1}[l,p]\right]^T\ , \end{aligned} \tag{4}$$

where

$$\begin{aligned} X_{1,n}[l,p] &= \sum_{i=0}^{L-1} x_{1,n}[L\cdot(p-1)+i]\cdot e^{-j\frac{2\pi}{L}il}\ , \\ X_{2,m}[l,p] &= \sum_{i=0}^{L-1} x_{2,m}[L\cdot(p-1)+i]\cdot e^{-j\frac{2\pi}{L}il}\ , \end{aligned} \tag{5}$$

with $p = 0, 1, \ldots, P-1$, and $l = 0, 1, \ldots, L-1$.

Define $S_k[l,p]$, $\overline{N}_{1,n}[l,p]$, and $\overline{N}_{2,m}[l,p]$ as the DFT of the p-th group discrete-time impinging signals $s_k[i]$, discrete-time noises at sensors of the two sub-arrays $\overline{n}_{1,n}[i]$ and $\overline{n}_{2,m}[i]$, respectively. $\mathbf{S}[l,p] = \left[S_1[l,p], \ldots, S_K[l,p]\right]^T$ is a column vector holding signals at the l-th frequency bin, and $\overline{\mathbf{N}}_1[l,p] = \left[\overline{N}_{1,0}[l,p], \ldots, \overline{N}_{1,N-1}[l,p]\right]^T$ and $\overline{\mathbf{N}}_2[l,p] =$

$\left[\overline{N}_{2,1}[l,p],\ldots,\overline{N}_{2,2M-1}[l,p]\right]^T$ are the corresponding column noise vectors at the two sub-arrays. Then, the output signal model in the DFT domain can be expressed as

$$\begin{aligned}\mathbf{X}_1[l,p] &= \mathbf{A}_1(l,\boldsymbol{\theta})\mathbf{S}[l,p] + \overline{\mathbf{N}}_1[l,p]\ ,\\ \mathbf{X}_2[l,p] &= \mathbf{A}_2(l,\boldsymbol{\theta})\mathbf{S}[l,p] + \overline{\mathbf{N}}_2[l,p]\ ,\end{aligned} \tag{6}$$

where $\mathbf{A}_1(l,\boldsymbol{\theta}) = [\mathbf{a}_1(l,\theta_1),\ldots,\mathbf{a}_1(l,\theta_K)]$ and $\mathbf{A}_2(l,\boldsymbol{\theta}) = [\mathbf{a}_2(l,\theta_1),\ldots,\mathbf{a}_2(l,\theta_K)]$ are the steering matrices at frequency f_l corresponding to the l-th frequency bin. The column vectors $\mathbf{a}_1(l,\theta_k)$ and $\mathbf{a}_2(l,\theta_k)$ are the steering vectors at frequency f_l and angle θ_k, given as

$$\begin{aligned}\mathbf{a}_1(l,\theta_k) &= \left[1, e^{-j\frac{2\pi Md}{\lambda_l}\sin(\theta_k)},\ldots,e^{-j\frac{2\pi M(N-1)d}{\lambda_l}\sin(\theta_k)}\right]^T,\\ \mathbf{a}_2(l,\theta_k) &= \left[e^{-j\frac{2\pi Nd}{\lambda_l}\sin(\theta_k)},\ldots,e^{-j\frac{2\pi N(2M-1)d}{\lambda_l}\sin(\theta_k)}\right]^T,\end{aligned} \tag{7}$$

where $\lambda_l = c/f_l$ and c is the wave speed. For each l of interest, (6) can be considered as a narrowband signal model.

III. Sparsity-Based Low-Complexity DOA Estimation for a Single Frequency

In this section, we first review the narrowband DOA estimation method for co-prime arrays proposed in [16], using the single-frequency model in (6) as an example in Subsection III-A, and then propose our two low-complexity DOA estimation methods in Subsections III-B and III-C.

A. Review of DOA estimation for narrowband co-prime arrays

We consider DOA estimation using the data at the l-th frequency bin. Denote $\mathbf{X}[l,p] = \left[\mathbf{X}_1^T[l,p], \mathbf{X}_2^T[l,p]\right]^T$. Then, the covariance matrix for $\mathbf{X}[l,p]$ is

$$\begin{aligned}\mathbf{R}_{\mathbf{xx}}[l] &= \mathrm{E}\left\{\mathbf{X}[l,p]\cdot\mathbf{X}^H[l,p]\right\}\\ &= \sum_{k=1}^{K}\sigma_k^2[l]\mathbf{a}(l,\theta_k)\mathbf{a}^H(l,\theta_k) + \sigma_{\bar{n}}^2[l]\mathbf{I}_{2M+N-1}\ ,\end{aligned} \tag{8}$$

where $\{\cdot\}^H$ denotes Hermitian transpose, $\mathrm{E}\{\cdot\}$ is the expectation operator, $\mathbf{a}(l,\theta_k) = \left[\mathbf{a}_1^T(l,\theta_k), \mathbf{a}_2^T(l,\theta_k)\right]^T$ and $\mathbf{I}_{2M+N-1}$ is the $(2M+N-1)\times(2M+N-1)$ identity matrix. $\sigma_k^2[l]$ represents the power of the k-th impinging signal at the l-th frequency bin, and $\sigma_{\bar{n}}^2[l]$ is the corresponding noise power.

In practice, $\mathbf{R}_{\mathbf{xx}}[l]$ can be estimated by

$$\mathbf{R}_{\mathbf{xx}}[l] \approx \widehat{\mathbf{R}}_{\mathbf{xx}}[l] = \frac{1}{P}\sum_{p=0}^{P-1}\mathbf{X}[l,p]\cdot\mathbf{X}^H[l,p]\ , \tag{9}$$

where P is the number of signal blocks for DFT and we assume that the impinging source signals are wide-sense stationary over this period.

Vectorizing $\mathbf{R}_{\mathbf{xx}}[l]$ yields

$$\mathbf{z}[l] = \mathrm{vec}\left\{\mathbf{R}_{\mathbf{xx}}[l]\right\} = \widetilde{\mathbf{A}}[l]\widetilde{\mathbf{s}}[l] + \sigma_{\bar{n}}^2[l]\widetilde{\mathbf{I}}_{2M+N-1}\ , \tag{10}$$

where $\widetilde{\mathbf{A}}[l] = [\widetilde{\mathbf{a}}(l,\theta_1),\ldots,\widetilde{\mathbf{a}}(l,\theta_K)]$ with $\widetilde{\mathbf{a}}(l,\theta_k) = \mathbf{a}^*(l,\theta_k)\otimes\mathbf{a}(l,\theta_k)$ ($\otimes$ is the Kronecker product and $\{\cdot\}^*$ denotes the conjugate operation), and $\widetilde{\mathbf{s}}[l] = \left[\sigma_1^2[l],\ldots,\sigma_K^2[l]\right]^T$. $\widetilde{\mathbf{I}}_{2M+N-1}$ is a $(2M+N-1)^2\times 1$ column vector obtained by vectorizing $\mathbf{I}_{2M+N-1}$.

Equation (10) characterises a virtual array with a higher number of DOFs, where $\widetilde{\mathbf{A}}[l]$ represents its steering matrix and $\widetilde{\mathbf{s}}[l]$ represents its equivalent impinging signal vector. Note that the increased DOFs are only available in the signal and noise power domain, which enable the DOA estimation of the signals, but cannot be used to recover their waveforms. $\widetilde{\mathbf{A}}[l]$ contains virtual sensor positions distributed in the set of cross differences

$$\left\{\pm(Nm-Mn)\cdot d, 0\le n\le N-1 \bigcap 1\le m\le 2M-1\right\}$$

and the two sets of self differences

$$\begin{aligned}&\{(Nm_1-Nm_2)\cdot d, 1\le m_1\le 2M-1, 1\le m_2\le 2M-1\}\ ,\\ &\{(Mn_1-Mn_2)\cdot d, 0\le n_1\le N-1, 0\le n_2\le N-1\}\ .\end{aligned}$$

Moreover, (10) can be modified into

$$\mathbf{z}[l] = \widetilde{\mathbf{A}}[l]\widetilde{\mathbf{s}}[l] + \sigma_{\bar{n}}^2[l]\widetilde{\mathbf{I}}_{2M+N-1} = \widetilde{\mathbf{A}}^{\circ}[l]\widetilde{\mathbf{s}}^{\circ}[l]\ , \tag{11}$$

where $\widetilde{\mathbf{A}}^{\circ}[l] = \left[\widetilde{\mathbf{A}}[l], \widetilde{\mathbf{I}}_{2M+N-1}\right]$ and $\widetilde{\mathbf{s}}^{\circ}[l] = \left[\widetilde{\mathbf{s}}^T[l], \sigma_{\bar{n}}^2[l]\right]^T$.

For the l-th frequency bin, with a search grid of K_g potential incident angles $\theta_{g,1},\ldots,\theta_{g,K_g}$, the steering matrix is generated by $\widetilde{\mathbf{A}}_{\mathbf{g}}[l] = \left[\widetilde{\mathbf{a}}(l,\theta_{g,1}),\ldots,\widetilde{\mathbf{a}}(l,\theta_{g,K_g})\right]$. Here we use the subscript $\{\cdot\}_g$ to describe matrices, vectors or elements related to the generated search grid. Construct a column vector $\widetilde{\mathbf{s}}_{\mathbf{g}}[l]$ consisting of K_g elements, each representing a potential source signal at the corresponding incident angle. Denote

$$\widetilde{\mathbf{A}}_{\mathbf{g}}^{\circ}[l] = \left[\widetilde{\mathbf{A}}_{\mathbf{g}}[l], \widetilde{\mathbf{I}}_{2M+N-1}\right],\ \widetilde{\mathbf{s}}_{\mathbf{g}}^{\circ}[l] = \left[\widetilde{\mathbf{s}}_{\mathbf{g}}[l], \sigma_{\bar{n}}^2[l]\right]^T. \tag{12}$$

The last element $\sigma_{\bar{n}}^2[l]$ in $\widetilde{\mathbf{s}}_{\mathbf{g}}^{\circ}[l]$ can also be considered as a variable because the noise power is unknown. All the elements in $\widetilde{\mathbf{s}}^{\circ}[l]$ are powers, and therefore positive real numbers. The method proposed in [16] can be applied to a single frequency in the wideband case directly with the following formulation

$$\begin{aligned}\min\quad & \left\|\widetilde{\mathbf{s}}_{\mathbf{g}}^{\circ}[l]\right\|_1\\ \text{subject to}\quad & \left\|\mathbf{z}[l] - \widetilde{\mathbf{A}}_{\mathbf{g}}^{\circ}[l]\widetilde{\mathbf{s}}_{\mathbf{g}}^{\circ}[l]\right\|_2 \le \varepsilon\ ,\\ & \widetilde{s}_{g,k_g}^{\circ}[l]\ge 0,\quad 0\le k_g\le K_g\ ,\end{aligned} \tag{13}$$

where ε is the allowable error bound, $\|\cdot\|_1$ is the l_1 norm and $\|\cdot\|_2$ the l_2 norm. $\widetilde{s}_{g,k_g}^{\circ}[l]$ represents the k_g-th entry in the column vector $\widetilde{\mathbf{s}}_{\mathbf{g}}^{\circ}[l]$.

B. Low-complexity DOA estimation for a single frequency

We first add the received signal of the zeroth sensor into the signal vector of the second sub-array. Then (4) changes to

$$\begin{aligned}\mathbf{X}_1[l,p] &= \left[X_{1,0}[l,p],\ldots,X_{1,N-1}[l,p]\right]^T,\\ \overline{\mathbf{X}}_2[l,p] &= \left[X_{2,0}[l,p],\ldots,X_{2,2M-1}[l,p]\right]^T,\end{aligned} \tag{14}$$

where $X_{2,0}[l,p] = X_{1,0}[l,p]$, and the steering vectors described in (7) become

$$\begin{aligned}\mathbf{a}_1(l,\theta_k) &= \left[1, e^{-j\frac{2\pi Md}{\lambda_l}\sin(\theta_k)},\ldots,e^{-j\frac{2\pi M(N-1)d}{\lambda_l}\sin(\theta_k)}\right]^T,\\ \overline{\mathbf{a}}_2(l,\theta_k) &= \left[1, e^{-j\frac{2\pi Nd}{\lambda_l}\sin(\theta_k)},\ldots,e^{-j\frac{2\pi N(2M-1)d}{\lambda_l}\sin(\theta_k)}\right]^T.\end{aligned} \tag{15}$$

Then, the auto-correlation matrices of the signal vectors observed in the two sub-arrays can be obtained as

$$\begin{aligned}\mathbf{R}_{11}[l] &= \mathrm{E}\left\{\mathbf{X}_1[l,p]\cdot\mathbf{X}_1^H[l,p]\right\}\\ &= \sum_{k=1}^{K}\sigma_k^2[l]\mathbf{a}_1[l,\theta_k]\mathbf{a}_1^H[l,\theta_k]+\sigma_{\bar{n}}^2[l]\mathbf{I}_N\ ,\end{aligned} \tag{16}$$

$$\begin{aligned}\mathbf{R}_{22}[l] &= \mathrm{E}\left\{\overline{\mathbf{X}}_2[l,p]\cdot\overline{\mathbf{X}}_2^H[l,p]\right\}\\ &= \sum_{k=1}^{K}\sigma_k^2[l]\overline{\mathbf{a}}_2[l,\theta_k]\overline{\mathbf{a}}_2^H[l,\theta_k]+\sigma_{\bar{n}}^2[l]\mathbf{I}_{2M}\ ,\end{aligned} \tag{17}$$

where $\mathbf{I}_N$ and $\mathbf{I}_{2M}$ are identity matrices with size of $N\times N$ and $2M\times 2M$, respectively. Note here that $\mathbf{R}_{11}[l]$ and $\mathbf{R}_{22}[l]$ are both Hermitian and Toeplitz.

We can also obtain the cross-correlation matrices of the two sub-arrays, given by

$$\begin{aligned}\mathbf{R}_{12}[l] &= \mathrm{E}\left\{\mathbf{X}_1[l,p]\cdot\overline{\mathbf{X}}_2^H[l,p]\right\}\\ &= \sum_{k=1}^{K}\sigma_k^2[l]\mathbf{a}_1[l,\theta_k]\overline{\mathbf{a}}_2^H[l,\theta_k]+\sigma_{\bar{n}}^2[l]\mathbf{W}_{N,2M}\ ,\end{aligned} \tag{18}$$

$$\begin{aligned}\mathbf{R}_{21}[l] &= \mathrm{E}\left\{\overline{\mathbf{X}}_2[l,p]\cdot\mathbf{X}_1^H[l,p]\right\}\\ &= \sum_{k=1}^{K}\sigma_k^2[l]\overline{\mathbf{a}}_2[l,\theta_k]\mathbf{a}_1^H[l,\theta_k]+\sigma_{\bar{n}}^2[l]\mathbf{W}_{2M,N}\ ,\end{aligned} \tag{19}$$

where $\mathbf{W}_{N,2M}$ has a size of $N\times 2M$ and $\mathbf{W}_{2M,N}$ has a size of $2M\times N$, both being all zeroes except for a value of 1 at the $(0,0)$th entry. We have $\mathbf{R}_{12}[l]=\mathbf{R}_{21}^H[l]$.

For $0\le n\le N-1$ and $0\le m\le 2M-1$, the set of cross difference $b=Nm-Mn$ can reach any integer in the range of 0 to MN [13], [14]. The cross difference sets of $b=Nm-Mn$ and $-b=-Nm+Mn$ also contain all the lags included in self difference sets provided by $\mathbf{R}_{11}$ and $\mathbf{R}_{22}$ [27]. The redundant lags can be combined together. Furthermore, the information contained in $\mathbf{R}_{21}[l]$ is the same as that in $\mathbf{R}_{12}[l]$. Therefore, the virtual array generated from $\mathbf{R}_{12}[l]$ contains all the degrees of freedom. In practice, $\mathbf{R}_{12}[l]$, $\mathbf{R}_{11}[l]$, and $\mathbf{R}_{22}[l]$ can be replaced by their finite-sample estimates $\widehat{\mathbf{R}}_{12}[l]$, $\widehat{\mathbf{R}}_{21}[l]$, $\widehat{\mathbf{R}}_{11}[l]$, and $\widehat{\mathbf{R}}_{22}[l]$, respectively.

Considering $\widehat{\mathbf{R}}_{11}[l]=\widehat{\mathbf{R}}_{11}^H[l]$, $\widehat{\mathbf{R}}_{22}[l]=\widehat{\mathbf{R}}_{22}^H[l]$, and $\widehat{\mathbf{R}}_{12}[l]=\widehat{\mathbf{R}}_{21}^H[l]$, the complex conjugate part in matrices $\widehat{\mathbf{R}}_{11}[l]$, $\widehat{\mathbf{R}}_{22}[l]$, and the entire matrix $\widehat{\mathbf{R}}_{21}[l]$ can be removed in virtual array generation for complexity reduction. A more accurate estimation of the virtual array model can be obtained by averaging all the entries with the same lag in auto-correlation matrices. Denote $\mathbf{R_c}[l]$ as the new cross-correlation matrix at the l-th frequency bin. Then, the entry in the n-th row and the m-th column of $\mathbf{R_c}[l]$ is expressed as

$$R_c^{n,m}[l]=\begin{cases}\dfrac{\sum\limits_{\hat{n}=0}^{N-1}\widehat{R}_{11}^{\hat{n},\hat{n}}[l]+\sum\limits_{\hat{m}=1}^{2M-1}\widehat{R}_{22}^{\hat{m},\hat{m}}[l]}{2M+N-1}, & n,m=0,\\ \dfrac{\sum\limits_{\hat{m}=m}^{2M-1}\widehat{R}_{22}^{\hat{m}-m,\hat{m}}[l]}{2M-m}, & n=0,m\neq 0,\\ \dfrac{\sum\limits_{\hat{n}=n}^{N-1}\widehat{R}_{11}^{\hat{n},\hat{n}-n}[l]}{N-n}, & n\neq 0,m=0,\\ \widehat{R}_{12}^{n,m}[l], & \text{others},\end{cases} \tag{20}$$

where the superscripts are the corresponding row and column indexes.

In (20), an accurate estimation of $\mathbf{R}_{12}$ is obtained by removing duplicate entries and combining redundant entries in $\mathbf{R}_{11}$ and $\mathbf{R}_{22}$. Furthermore, redundant entries in $\mathbf{R}_{12}$ can also be combined for further complexity reduction.

The n-th row and m-th column entry in $\mathbf{R}_{12}$ is

$$R_{12}^{n,m}[l]=\begin{cases}\sum\limits_{k=1}^{K}\sigma_k^2[l]e^{-j\frac{2\pi(nM-mN)d}{\lambda_l}\sin(\theta_k)}+\sigma_{\bar{n}}^2[l], & m=n=0,\\ \sum\limits_{k=1}^{K}\sigma_k^2[l]e^{-j\frac{2\pi(nM-mN)d}{\lambda_l}\sin(\theta_k)}, & \text{others}.\end{cases} \tag{21}$$

Signal powers $\sigma_k^2[l], k=1,2,\cdots,K$, and noise power $\sigma_{\bar{n}}^2[l]$ are all positive real numbers. Considering indexes of (n_1,m_1) and (n_2,m_2), $R_{12}^{n_1,m_1}[l]$ and $R_{12}^{n_2,m_2}[l]$ are complex conjugate when the indexes satisfy the following relationship

$$n_1M-m_1N=-(n_2M-m_2N)\ ,$$

which can be modified as

$$(n_1+n_2)M=(m_1+m_2)N\ , \tag{22}$$

where $0\le n_1\le N-1$, $0\le n_2\le N-1$, $0\le m_1\le 2M-1$, and $0\le m_2\le 2M-1$. Then, the only necessary and sufficient condition of (22) is

$$n_1+n_2=N\bigcap m_1+m_2=M\ . \tag{23}$$

Thus, we can obtain the following relationship in matrix $\mathbf{R}_{12}$

$$R_{12}^{n_1,m_1}[l]=\left\{R_{12}^{n_2,m_2}[l]\right\}^*=\left\{R_{12}^{N-n_1,M-m_1}[l]\right\}^*, \tag{24}$$

where $1\le(n_1,n_2)\le N-1$ and $0\le(m_1,m_2)\le M$.

In practice, $\mathbf{R}_{12}[l]$ is replaced by $\widehat{\mathbf{R}}_{12}[l]$, and a more accurate estimation of the smoothed cross-correlation matrix can be obtained by averaging the conjugate entries, with (20)

updated to

$$\bar{R}_c^{n,m}[l] = \begin{cases} \dfrac{\sum_{\hat{n}=0}^{N-1}\widehat{R}_{11}^{\hat{n},\hat{n}}[l]+\sum_{\hat{m}=1}^{2M-1}\widehat{R}_{22}^{\hat{m},\hat{m}}[l]}{2M+N-1}, & n,m=0, \\ \dfrac{\sum_{\hat{m}=m}^{2M-1}\widehat{R}_{22}^{\hat{m}-m,\hat{m}}[l]}{2M-m}, & n=0,m\neq 0, \\ \dfrac{\sum_{\hat{n}=n}^{N-1}\widehat{R}_{11}^{\hat{n},\hat{n}-n}[l]+\left\{\widehat{R}_{12}^{N-n,M-m}\right\}^*}{N-n+1}, & n\neq 0,m=0, \\ \dfrac{\left\{\sum_{\hat{n}=N-n}^{N-1}\widehat{R}_{11}^{\hat{n},\hat{n}-N+n}[l]\right\}^*+\widehat{R}_{12}^{n,m}}{n+1}, & n\neq 0,m=M, \\ \dfrac{\widehat{R}_{12}^{n,m}+\left\{\widehat{R}_{12}^{N-n,M-m}\right\}^*}{2}, & n\neq 0,1\leq m<M, \\ \widehat{R}_{12}^{n,m}[l], & \text{others}, \end{cases} \tag{25}$$

where $\bar{R}_c^{n,m}[l]$ is the n-th row and the m-th column entry in the updated smoothed cross-correlation matrix $\overline{\mathbf{R}}_{\mathbf{c}}^{n,m}[l]$.

Matrix $\overline{\mathbf{R}}_{\mathbf{c}}[l]$ corresponds to the cross difference co-array $-b = Mn - Nm$, with the ability of reaching all the integers in the range of $-MN$ to 0, where $0 \leq n \leq N-1$ and $0 \leq m \leq 2M-1$. According to (21) and (25), the positive lags in the cross difference co-array $-b = Mn - Nm$ have been combined and can be removed when vectorizing $\overline{\mathbf{R}}_{\mathbf{c}}[l]$, and the number of positive lags is $\frac{(N-1)(M+1)}{2}$.

$\bar{\mathbf{z}}_{\mathbf{c}}[l]$ is the vector obtained by vectorizing $\overline{\mathbf{R}}_{\mathbf{c}}[l]$, i.e.

$$\begin{aligned} \bar{\mathbf{z}}_{\mathbf{c}}[l] &= \operatorname{vec}\left\{\overline{\mathbf{R}}_{\mathbf{c}}[l]\right\} \\ &= \widetilde{\mathbf{A}}_{\mathbf{c}}[l]\widetilde{\mathbf{s}}[l] + \sigma_{\bar{n}}^2[l]\widetilde{\mathbf{w}}_{N,2M} = \widetilde{\mathbf{A}}_{\mathbf{c}}^{\circ}[l]\widetilde{\mathbf{s}}^{\circ}[l] \,, \end{aligned} \tag{26}$$

where $\widetilde{\mathbf{A}}_{\mathbf{c}}[l] = \left[\widetilde{\mathbf{a}}_{\mathbf{c}}[l,\theta_1],\ldots,\widetilde{\mathbf{a}}_{\mathbf{c}}[l,\theta_K]\right]$ with $\widetilde{\mathbf{a}}_{\mathbf{c}}[l,\theta_k] = \bar{\mathbf{a}}_2^*[l,\theta_k]\otimes\mathbf{a}_1[l,\theta_k]$, and $\widetilde{\mathbf{s}}[l] = \left[\sigma_1^2[l],\ldots,\sigma_K^2[l]\right]^T$. $\widetilde{\mathbf{w}}_{N,2M}$ is a $2MN\times 1$ column vector obtained by vectorizing the matrix $\mathbf{W}_{N,2M}$. $\widetilde{\mathbf{A}}_{\mathbf{c}}^{\circ}[l]$ and $\widetilde{\mathbf{s}}^{\circ}[l]$ are given as

$$\widetilde{\mathbf{A}}_{\mathbf{c}}^{\circ}[l] = \left[\widetilde{\mathbf{A}}_{\mathbf{c}}[l], \widetilde{\mathbf{w}}_{N,2M}\right], \ \widetilde{\mathbf{s}}^{\circ}[l] = \left[\widetilde{\mathbf{s}}^T[l], \sigma_{\bar{n}}^2[l]\right]^T. \tag{27}$$

With the same search grid of K_g potential angles $\theta_{g,1},\ldots,\theta_{g,K_g}$ as used earlier, the steering matrix is generated by $\widetilde{\mathbf{A}}_{\mathbf{cg}}[l] = \left[\widetilde{\mathbf{a}}_{\mathbf{c}}[l,\theta_{g,1}],\ldots,\widetilde{\mathbf{a}}_{\mathbf{c}}[l,\theta_{g,K_g}]\right]$. Construct a K_g-element column vector $\widetilde{\mathbf{s}}_{\mathbf{g}}[l]$, with each element representing a potential source at the corresponding incident angle. Denote

$$\widetilde{\mathbf{A}}_{\mathbf{cg}}^{\circ}[l] = \left[\widetilde{\mathbf{A}}_{\mathbf{cg}}[l], \widetilde{\mathbf{W}}_{N,2M}\right] \ , \ \widetilde{\mathbf{s}}_{\mathbf{g}}^{\circ}[l] = \left[\widetilde{\mathbf{s}}_{\mathbf{g}}^T[l], \sigma_{\bar{n}}^2[l]\right]^T \ . \tag{28}$$

We use n_c, $0 \leq n_c \leq 2MN-1$, to denote the row index of the column vector $\bar{\mathbf{z}}_{\mathbf{c}}[l]$, the matrix $\widetilde{\mathbf{A}}_{\mathbf{c}}[l]$ in (26), and the matrix $\widetilde{\mathbf{A}}_{\mathbf{cg}}[l]$ in (28). Then, each entry of $\bar{\mathbf{z}}_{\mathbf{c}}[l]$ is expressed as $\bar{z}_{n_c}[l]$. Row vectors $\widetilde{\mathbf{a}}_{\mathbf{c},n_c}[l]$ and $\widetilde{\mathbf{a}}_{\mathbf{cg},n_c}[l]$ are used to represent the n_c-th row of the matrices $\widetilde{\mathbf{A}}_{\mathbf{c}}[l]$ and $\widetilde{\mathbf{A}}_{\mathbf{cg}}[l]$, respectively. Denote $n_{c,n_0}\in\Phi, n_0 = 0,1,\cdots,N_0-1$, as the row indexes corresponding to all the negative lags, where $N_0 = 2MN - \frac{(N-1)(M+1)}{2}$ is the number of indexes set $\Phi = \{Nm+n, 0 \leq n \leq N-1 \bigcap 0 \leq m \leq 2M-1 \bigcap Mn-Nm \leq 0\}$. Keeping all the row indexes n_{c,n_0}, we obtain a virtual array model as

$$\check{\mathbf{z}}_{\mathbf{c}}[l] = \check{\mathbf{A}}_{\mathbf{c}}^{\circ}[l]\widetilde{\mathbf{s}}^{\circ}[l] \,, \tag{29}$$

where $\check{\mathbf{z}}_{\mathbf{c}}[l] = \left[\bar{z}_{n_{c,0}}[l],\cdots,\bar{z}_{n_{c,N_0-1}}[l]\right]^T$ and $\check{\mathbf{A}}_{\mathbf{c}}^{\circ}[l] = \left[\widetilde{\mathbf{a}}_{\mathbf{c},n_{c,0}}^T[l],\cdots,\widetilde{\mathbf{a}}_{\mathbf{c},n_{c,N_0-1}}^T[l]\right]^T$.

Then the proposed low-complexity DOA estimation method can be expressed as

$$\begin{aligned} \min \quad & \left\|\widetilde{\mathbf{s}}_{\mathbf{g}}^{\circ}[l]\right\|_1 \\ \text{subject to} \quad & \left\|\check{\mathbf{z}}_{\mathbf{c}}[l] - \check{\mathbf{A}}_{\mathbf{cg}}^{\circ}[l]\widetilde{\mathbf{s}}_{\mathbf{g}}^{\circ}[l]\right\|_2 \leq \varepsilon \,, \\ & \widetilde{s}_{g,k_g}^{\circ}[l] \geq 0, \quad 0 \leq k_g \leq K_g \,, \end{aligned} \tag{30}$$

where $\check{\mathbf{A}}_{\mathbf{cg}}^{\circ}[l] = \left[\widetilde{\mathbf{a}}_{\mathbf{cg},n_{c,0}}^T[l],\cdots,\widetilde{\mathbf{a}}_{\mathbf{cg},n_{c,N_0-1}}^T[l]\right]^T$, and $\widetilde{s}_{g,k_g}[l]$ is the k_g-th entry of column vector $\widetilde{\mathbf{s}}_{\mathbf{g}}[l]$.

In (13) and (30), the first K_g elements of $\widetilde{\mathbf{s}}_{\mathbf{g}}^{\circ}[l]$ give the corresponding DOA estimation results over K_g search grids. Compared with (13), there is a significant reduction in the number of entries in the optimization problem (30) due to the combination of redundant entries, leading to reduction in computational complexity using various optimisation toolboxes.

C. Further reduction by removing noise power estimation

In (26), $\widetilde{\mathbf{w}}_{N,2M}$ is an all-zero column vector except for the zeroth entry. Only the zeroth element in $\check{\mathbf{z}}_{\mathbf{c}}[l]$ related to the zero lag is influenced by noise power $\sigma_{\bar{n}}^2[l]$, and the estimation of noise power takes up one DOF. As a result, we can remove the zero lag part to avoid estimating $\sigma_{\bar{n}}^2[l]$ in (30). In so doing, the range of difference co-array lags in $\overline{\mathbf{R}}_{\mathbf{c}}[l]$ from $-MN$ to -1 with MN DOFs can still be provided by the co-prime array, with the new set of available DOFs fully dedicated to DOA estimation. Further reduction in computational complexity is achieved due to the reduction in the number of parameters to be estimated and the number of entries.

We use n_0, $0 \leq n_0 \leq N_0-1$, to be the row index of $\check{\mathbf{z}}_{\mathbf{c}}[l]$, $\check{\mathbf{A}}_{\mathbf{c}}[l]$ in (29), and $\check{\mathbf{A}}_{\mathbf{cg}}[l]$ in (30). Then, each entry of $\check{\mathbf{z}}_{\mathbf{c}}[l]$ is expressed as $\check{z}_{c,n_0}[l]$. Row vectors $\check{\mathbf{a}}_{\mathbf{cr},n_0}[l]$ and $\check{\mathbf{a}}_{\mathbf{cg},n_0}[l]$ are used to represent the n_0-th row of $\check{\mathbf{A}}_{\mathbf{c}}[l]$ and $\check{\mathbf{A}}_{\mathbf{cg}}[l]$, respectively. Removing the first row with $n_0 = 0$, we obtain a virtual array model

$$\mathbf{z}_{\mathbf{s}}[l] = \widetilde{\mathbf{A}}_{\mathbf{s}}[l]\widetilde{\mathbf{s}}[l] \,, \tag{31}$$

where $\mathbf{z}_{\mathbf{s}}[l] = \left[\check{z}_{c,1}[l],\cdots,\check{z}_{c,N_0-1}[l]\right]^T$, and $\widetilde{\mathbf{A}}_{\mathbf{s}}[l] = \left[\check{\mathbf{a}}_{\mathbf{cr},1}^T[l],\cdots,\check{\mathbf{a}}_{\mathbf{cr},N_0-1}^T[l]\right]^T$.

Then, the modified low-complexity DOA estimation method for a single frequency at the l-th frequency bin can be expressed as

$$\begin{aligned} \min \quad & \left\|\widetilde{\mathbf{s}}_{\mathbf{g}}[l]\right\|_1 \\ \text{subject to} \quad & \left\|\mathbf{z}_{\mathbf{s}}[l] - \widetilde{\mathbf{A}}_{\mathbf{sg}}[l]\widetilde{\mathbf{s}}_{\mathbf{g}}[l]\right\|_2 \leq \varepsilon \\ & \widetilde{s}_{g,k_g}[l] \geq 0, \quad 0 \leq k_g \leq K_g - 1 \,, \end{aligned} \tag{32}$$

where $\widetilde{\mathbf{A}}_{\mathbf{sg}}[l] = \left[\check{\mathbf{a}}_{\mathbf{cg},1}^T[l],\cdots,\check{\mathbf{a}}_{\mathbf{cg},N_0-1}^T[l]\right]^T$, and $\widetilde{s}_{g,k_g}[l]$ is the k_g-th entry of the column vector $\widetilde{\mathbf{s}}_{\mathbf{g}}[l]$.

The problems in (13), (30), and (32) can be solved using CVX, a software package for specifying and solving convex problems [28], [29].

IV. Wideband DOA Estimation Method Based on Group Sparsity for Co-prime Arrays

For wideband signals transformed into multiple frequency bins as described in Section II, we could apply the algorithm in (13), (30), and (32) to the frequency range of interest one by one and then average the results to give the final estimation. A more effective approach that achieves a higher accuracy, however, is to jointly estimate the DOA of the impinging signals across the entire frequency range of interest simultaneously based on the group sparsity concept, i.e., the DOA results corresponding to different frequencies share the same spatial support, although they may have varying power values. Assume that the frequency range or bandwidth of interest covers Q frequency bins in the DFT domain, where the $Q \leq L$ frequency bins may or may not be adjacent to each other. For each frequency bin $l_q \in \Phi_l$, $0 \leq q \leq Q-1$, where Φ_l is the set of Q frequency bin indexes, the same search grid of K_g potential incident angles are used to generate all the matrices needed as described for each method.

A. Wideband extension 1 based on existing DOA estimation method

First, we construct two matrices: a block diagonal matrix $\widetilde{\mathbf{B}}_{\mathbf{g}}^{\circ}$ using $\widetilde{\mathbf{A}}_{\mathbf{g}}^{\circ}[l_q]$, expressed as

$$\widetilde{\mathbf{B}}_{\mathbf{g}}^{\circ} = \text{blkdiag}\left\{\widetilde{\mathbf{A}}_{\mathbf{g}}^{\circ}[l_0], \widetilde{\mathbf{A}}_{\mathbf{g}}^{\circ}[l_1], \ldots, \widetilde{\mathbf{A}}_{\mathbf{g}}^{\circ}[l_{Q-1}]\right\} \tag{33}$$

and a $(K_g+1) \times Q$ matrix $\mathbf{R}_{\mathbf{g}}^{\circ}$ using $\widetilde{\mathbf{s}}_{\mathbf{g}}^{\circ}[l_q]$ with

$$\mathbf{R}_{\mathbf{g}}^{\circ} = \left[\widetilde{\mathbf{s}}_{\mathbf{g}}^{\circ}[l_0], \widetilde{\mathbf{s}}_{\mathbf{g}}^{\circ}[l_1], \ldots, \widetilde{\mathbf{s}}_{\mathbf{g}}^{\circ}[l_{Q-1}]\right] . \tag{34}$$

Then, we obtain the following virtual array model

$$\widetilde{\mathbf{z}} = \widetilde{\mathbf{B}}_{\mathbf{g}}^{\circ}\widetilde{\mathbf{r}}_{\mathbf{g}}^{\circ} , \tag{35}$$

where $\widetilde{\mathbf{z}} = \left[\mathbf{z}^T[l_0], \ldots, \mathbf{z}^T[l_{Q-1}]\right]^T$ and $\widetilde{\mathbf{r}}_{\mathbf{g}}^{\circ} = \text{vec}\left(\mathbf{R}_{\mathbf{g}}^{\circ}\right)$ is a $(K_g+1)\cdot Q \times 1$ column vector by vectorizing $\mathbf{R}_{\mathbf{g}}^{\circ}$.

We use the row vector $\mathbf{r}_{\mathbf{g},k_g}^{\circ}$, $0 \leq k_0 \leq K_g$, to represent the k_0-th row of the matrix $\mathbf{R}_{\mathbf{g}}^{\circ}$. Then, we form a new $(K_g+1)\times 1$ vector $\hat{\mathbf{r}}_{\mathbf{g}}^{\circ}$ based on the l_2 norm of $\mathbf{r}_{\mathbf{g},k_0}^{\circ}$, $0 \leq k_0 \leq K_g$

$$\hat{\mathbf{r}}_{\mathbf{g}}^{\circ} = \left[\left\|\mathbf{r}_{\mathbf{g},0}^{\circ}\right\|_2, \ldots, \left\|\mathbf{r}_{\mathbf{g},K_g}^{\circ}\right\|_2\right]^T . \tag{36}$$

Finally, our group-sparsity based wideband DOA estimation method is formulated as follows

$$\begin{aligned} \min_{\widetilde{\mathbf{r}}_{\mathbf{g}}^{\circ}} \quad & \left\|\hat{\mathbf{r}}_{\mathbf{g}}^{\circ}\right\|_1 \\ \text{subject to} \quad & \left\|\widetilde{\mathbf{z}} - \widetilde{\mathbf{B}}_{\mathbf{g}}^{\circ}\widetilde{\mathbf{r}}_{\mathbf{g}}^{\circ}\right\|_2 \leq \varepsilon , \\ & \widetilde{r}_{g,k_g}^{\circ} \geq 0, \quad 0 \leq k_g \leq (K_g+1)\cdot Q - 1 , \end{aligned} \tag{37}$$

where $\widetilde{r}_{g,k_g}^{\circ}$ represents the k_g-th element of the column vector $\widetilde{\mathbf{r}}_{\mathbf{g}}^{\circ}$, and the nonzero entries in the first K_g elements of the column vector $\hat{\mathbf{r}}_{\mathbf{g}}^{\circ}$ are the corresponding wideband DOA estimation results over the K_g search grids.

B. Wideband extension 2 based on proposed low-complexity DOA estimation method

The proposed low-complexity wideband virtual array model extended from narrowband DOA estimation method (30) can be shown as

$$\check{\mathbf{z}}_{\mathbf{c}}^{\circ} = \check{\mathbf{B}}_{\mathbf{cg}}^{\circ}\widetilde{\mathbf{r}}_{\mathbf{g}}^{\circ} , \tag{38}$$

where $\check{\mathbf{z}}_{\mathbf{c}}^{\circ} = \left[\mathbf{z}_{\mathbf{c}}^T[l_0], \ldots, \mathbf{z}_{\mathbf{c}}^T[l_{Q-1}]\right]^T$, $\widetilde{\mathbf{r}}_{\mathbf{g}}^{\circ} = \text{vec}\left(\mathbf{R}_{\mathbf{g}}^{\circ}\right)$, and the block diagonal matrix $\check{\mathbf{B}}_{\mathbf{cg}}^{\circ}$ given by

$$\check{\mathbf{B}}_{\mathbf{cg}}^{\circ} = \text{blkdiag}\left\{\check{\mathbf{A}}_{\mathbf{cg}}^{\circ}[l_0], \check{\mathbf{A}}_{\mathbf{cg}}^{\circ}[l_1], \ldots, \check{\mathbf{A}}_{\mathbf{cg}}^{\circ}[l_{Q-1}]\right\} . \tag{39}$$

Then, the proposed low-complexity wideband DOA estimation method is formulated as

$$\begin{aligned} \min_{\widetilde{\mathbf{r}}_{\mathbf{g}}^{\circ}} \quad & \left\|\hat{\mathbf{r}}_{\mathbf{g}}^{\circ}\right\|_1 \\ \text{subject to} \quad & \left\|\check{\mathbf{z}}_{\mathbf{c}}^{\circ} - \check{\mathbf{B}}_{\mathbf{cg}}^{\circ}\widetilde{\mathbf{r}}_{\mathbf{g}}^{\circ}\right\|_2 \leq \varepsilon , \\ & \widetilde{r}_{g,k_g}^{\circ} \geq 0, \quad 0 \leq k_g \leq (K_g+1)\cdot Q - 1 , \end{aligned} \tag{40}$$

C. Wideband extension 3 based on further complexity reduction DOA estimation method

Two matrices, i.e., block diagonal matrix $\widetilde{\mathbf{B}}_{\mathbf{sg}}$ and $K_g \times Q$ matrix $\mathbf{R}_{\mathbf{g}}$, are constructed using $\widetilde{\mathbf{A}}_{\mathbf{sg}}[l_q]$ and $\widetilde{\mathbf{s}}_{\mathbf{g}}[l_q]$ respectively, given by

$$\begin{aligned} \widetilde{\mathbf{B}}_{\mathbf{sg}} &= \text{blkdiag}\left\{\widetilde{\mathbf{A}}_{\mathbf{sg}}[l_0], \widetilde{\mathbf{A}}_{\mathbf{sg}}[l_1], \ldots, \widetilde{\mathbf{A}}_{\mathbf{sg}}[l_{Q-1}]\right\} , \\ \mathbf{R}_{\mathbf{g}} &= \left[\widetilde{\mathbf{s}}_{\mathbf{g}}[l_0], \widetilde{\mathbf{s}}_{\mathbf{g}}[l_1], \ldots, \widetilde{\mathbf{s}}_{\mathbf{g}}[l_{Q-1}]\right] . \end{aligned} \tag{41}$$

Then, the further improved wideband virtual array model is given by

$$\widetilde{\mathbf{z}}_{\mathbf{s}} = \widetilde{\mathbf{B}}_{\mathbf{sg}}\widetilde{\mathbf{r}}_{\mathbf{g}} , \tag{42}$$

where $\widetilde{\mathbf{z}}_{\mathbf{s}} = \left[\mathbf{z}_{\mathbf{s}}^T[l_0], \ldots, \mathbf{z}_{\mathbf{s}}^T[l_{Q-1}]\right]^T$ and $\widetilde{\mathbf{r}}_{\mathbf{g}} = \text{vec}\left(\mathbf{R}_{\mathbf{g}}\right)$ is a $K_g \cdot Q \times 1$ column vector by vectorizing $\mathbf{R}_{\mathbf{g}}$.

Row vector $\mathbf{r}_{\mathbf{g},k_0}$, $0 \leq k_0 \leq K_g - 1$ is used to represent the k_0-th row of $\mathbf{R}_{\mathbf{g}}$. Then, we form a new $K_g \times 1$ vector $\hat{\mathbf{r}}_{\mathbf{g}}$ based on the l_2 norm of $\mathbf{r}_{\mathbf{g},k_0}$, $0 \leq k_0 \leq K_g - 1$, as

$$\hat{\mathbf{r}}_{\mathbf{g}} = \left[\left\|\mathbf{r}_{\mathbf{g},0}\right\|_2, \left\|\mathbf{r}_{\mathbf{g},1}\right\|_2, \ldots, \left\|\mathbf{r}_{\mathbf{g},K_g-1}\right\|_2\right]^T . \tag{43}$$

Finally, the modified wideband DOA estimation method based on group sparsity is formulated as follows

$$\begin{aligned} \min_{\widetilde{\mathbf{r}}_{\mathbf{g}}} \quad & \left\|\hat{\mathbf{r}}_{\mathbf{g}}\right\|_1 \\ \text{subject to} \quad & \left\|\widetilde{\mathbf{z}}_{\mathbf{s}} - \widetilde{\mathbf{B}}_{\mathbf{sg}}\widetilde{\mathbf{r}}_{\mathbf{g}}\right\|_2 \leq \varepsilon , \\ & \widetilde{r}_{g,k_g} \geq 0, \quad 0 \leq k_g \leq K_g \cdot Q - 1 , \end{aligned} \tag{44}$$

where $\widetilde{r}_{g,k_g}$ represents the k_g-th element of the column vector $\widetilde{\mathbf{r}}_{\mathbf{g}}$, and the nonzero entries in the K_g elements of the column vector $\hat{\mathbf{r}}_{\mathbf{g}}$ are the corresponding wideband DOA estimation results over the K_g search grids.

Similar to the single frequency case, the reduction in the number of entries in the proposed wideband formulation will result in significant complexity reduction in the optimisation process. These optimization problems in (37), (40), and (44) can also be solved using CVX [28], [29].

D. Performance improvement with large unit spacing

The resolution of an array will improve with an increased aperture size. For existing DOA estimation methods for both narrowband signals and wideband signals, an equivalent unit spacing satisfying $d \leq \lambda_{\min}/2$ is normally chosen to avoid spatial aliasing. An advantage of our proposed group sparsity based methods is that we can increase the spacing d to be larger than $\lambda_{\min}/2$, while still avoiding spatial aliasing. This is because aliasing locations for different frequencies are different and the proposed group sparsity based methods will force a common sparsity location across all frequencies, corresponding to the true location of the impinging signals. Thus, the proposed methods allow a larger spacing than the standard co-prime array, leading to a larger virtual array aperture, and therefore more accurate estimation results can be obtained. However, we can expect that when d is larger than some threshold value, the DOA estimation results will degrade, as will be shown in our simulations part. When $d = \lambda_{\max}/2$, where the largest virtual array aperture can be achieved under the condition of no spatial aliasing only for the minimum frequency of interest, we can still perform effective DOA estimation.

V. Simulation Results

Consider a co-prime array with $M = 3$ and $N = 5$. With f_s twice the highest frequency of interest, the normalized frequencies of the impinging signals cover the range from 0.5π to π, and the unit spacing $d = \lambda_{\min}/2$ with $\lambda_{\min} = 2c/f_s$. As an example, for a microphone array, this is equivalent to a frequency band from 5 kHz to 10 kHz with a sampling frequency of 20 kHz and $\lambda_{\min} = 3.4$ cm at a speed of 340 m/s.

The number of signal samples in the time domain at each sensor is 128000, and DFT of $L = 64$ points is applied. Then, the number of data blocks used for estimating $\mathbf{R}_{\mathbf{xx}}[l]$, $\mathbf{R}_{11}[l]$, $\mathbf{R}_{22}[l]$, $\mathbf{R}_{12}[l]$, and $\mathbf{R}_{21}[l]$ at each frequency bin is $P = 2000$. There are 15 uncorrelated wideband signals impinging on the array, with incident angles uniformly distributed between -60° and 60°. A search grid of $K_g = 3601$ angles is formed within the full angle range with a step size of 0.05°. The normalized frequency range of impinging signals covers the frequency bin set $\Phi_l = \{17, 18, \cdots, 31\}$ with $Q = 15$.

A. Data Storage Analysis and Computation Time Comparison

First, the number of entries in the vectors/matrices involved is shown in Table I for the three narrowband DOA estimation methods and their wideband extensions. Fewer entries lead to less multiplicative and additive operations in the corresponding formulations, which is then translated into a lower computational complexity. For the underlying example, the exact number of entries is shown in Table II. We see that the existing method in (13) has the largest number of entries among all narrowband methods, while its wideband extension (37) has the largest number of entries among all wideband ones. The computation time using the CVX package, calculated by the MATLAB profiler under the environment of Intel CPU I5-3470 with a clock speed of 3.20GHz and 8GB RAM, is also listed in Table II. It is clear that the existing method has the longest processing time among all the three narrowband methods, with the one in (32) being the shortest. Their wideband extensions keep the same features.

B. Low-complexity DOA estimation results

For the first set of simulations, the input SNR is 0 dB and the allowable error bound ε is chosen to give the best result for each method through trial-and-error in every experiment[1]. Specifically, it is set to be 10 for the existing narrowband method in (13), 5 for our proposed low-complexity method in (30), and 4 for our modified method in (32). For the wideband case, 65, 25, and 13 were chosen as the allowable error bound ε, respectively. The much larger value for ε in the wideband case is due to the norm operation based on $Q = 15$ frequencies instead of one single frequency. The DOA estimation results for the single frequency ($l = 31$) are shown in Fig. 2, and the wideband results are shown in Fig. 3, where the dotted lines in the figures represent the actual incident angles of the impinging signals, while the solid lines represent the estimation results. It is clear that all the sources have been distinguished successfully by all the studied methods.

To compare the estimation accuracy with respect to a varied input SNR, the root mean square error (RMSE) results are shown in Fig. 4, where each point is based on an average of the results obtained by 500 simulation runs. Clearly, their narrowband performances are nearly the same for most of the cases, and their wideband extensions share a similar performance with extensions 2 and 3 being slightly more accurate. Furthermore, these proposed wideband extensions consistently outperform the narrowband ones by a large margin.

Finally, in this part, we give an example where the narrowband method clearly fails while the proposed wideband method can still provide a good result. The setting is the same as before except that now there are 21 sources uniformly distributed between -60° and 60°. Due to the increased signal number and reduced separation between DOAs of adjacent signals, the estimation task is much tougher than the previous settings and therefore can show the difference of their performances more effectively. The results of the modified low-complexity method for the single frequency case and its wideband extension are shown in Fig. 5, which again verifies the superior performance of the wideband method.

C. Results with large unit spacing co-prime arrays

Now we increase the unit spacing d to be larger than $\lambda_{\min}/2$, with $d = d_f \cdot \lambda_{\min}/2 = d_f \cdot c/f_s$, and examine its effect on the estimation results. To depict the change of the estimation results due to a change of d_f more clearly, a search grid of $K_g = 18001$ incident angles is formed within the full angle range with a smaller step size of 0.01°. Other parameters

[1]Roughly speaking, the value of ε is related to the noise power of the system and also all kinds of array and data model errors in the sparse reconstruction equation. Unfortunately, as a common parameter for all sparsity based optimisation methods, there is no analytical result for its selection for the general case and it is very difficult to give the range of this parameter for our simulation scenarios.

TABLE I
NUMBER OF ENTRIES IN VECTORS/MATRICES

Vector / Matrix	Methods for a Single Frequency		
	Existing (13)	Proposed (30)	Modified (32)
$\widetilde{\mathbf{s}}^{\circ}_{\mathbf{g}}[l]$ / $\widetilde{\mathbf{s}}^{\circ}_{\mathbf{g}}[l]$ / $\widetilde{\mathbf{s}}_{\mathbf{g}}[l]$	K_g+1	K_g+1	K_g
$\mathbf{z}[l]$ / $\check{\mathbf{z}}_{\mathbf{c}}[l]$ / $\mathbf{z}_{\mathbf{s}}[l]$	$(2M+N-1)^2$	$\frac{3MN-N+M+1}{2}$	$\frac{3MN-N+M-1}{2}$
$\widetilde{\mathbf{A}}^{\circ}_{\mathbf{g}}[l]$ / $\check{\mathbf{A}}^{\circ}_{\mathbf{cg}}[l]$ / $\widetilde{\mathbf{A}}_{\mathbf{sg}}[l]$	$(2M+N-1)^2(K_g+1)$	$\frac{(3MN-N+M+1)(K_g+1)}{2}$	$\frac{(3MN-N+M-1)K_g}{2}$
Vector / Matrix	Wideband DOA Estimation Methods		
	Extension 1 (37)	Extension 2 (40)	Extension 3 (44)
$\widetilde{\mathbf{r}}^{\circ}_{\mathbf{g}}$ / $\widetilde{\mathbf{r}}^{\circ}_{\mathbf{g}}$ / $\widetilde{\mathbf{r}}_{\mathbf{g}}$	$(K_g+1)Q$	$(K_g+1)Q$	$K_g \cdot Q$
$\widetilde{\mathbf{z}}$ / $\check{\mathbf{z}}^{\circ}_{\mathbf{c}}$ /$\widetilde{\mathbf{z}}_{\mathbf{s}}$	$(2M+N-1)^2 \cdot Q$	$\frac{(3MN-N+M+1)Q}{2}$	$\frac{(3MN-N+M-1)Q}{2}$
$\widetilde{\mathbf{B}}^{\circ}_{\mathbf{g}}$ / $\check{\mathbf{B}}^{\circ}_{\mathbf{cg}}$ / $\widetilde{\mathbf{B}}_{\mathbf{sg}}$	$(2M+N-1)^2(K_g+1)Q^2$	$\frac{(3MN-N+M+1)(K_g+1)Q^2}{2}$	$\frac{(3MN-N+M-1)K_gQ^2}{2}$

TABLE II
NUMBER OF ENTRIES IN VECTORS/MATRICES AND COMPUTATION TIME FOR THE EXAMPLE

Vector / Matrix	Methods for a Single Frequency		
	Existing (13)	Proposed (30)	Modified (32)
$\widetilde{\mathbf{s}}^{\circ}_{\mathbf{g}}[l]$ / $\widetilde{\mathbf{s}}^{\circ}_{\mathbf{g}}[l]$ / $\widetilde{\mathbf{s}}_{\mathbf{g}}[l]$	3602	3602	3601
$\mathbf{z}[l]$ / $\check{\mathbf{z}}_{\mathbf{c}}[l]$ / $\mathbf{z}_{\mathbf{s}}[l]$	100	22	21
$\widetilde{\mathbf{A}}^{\circ}_{\mathbf{g}}[l]$ / $\check{\mathbf{A}}^{\circ}_{\mathbf{cg}}[l]$ / $\widetilde{\mathbf{A}}_{\mathbf{sg}}[l]$	360200	79244	75621
Computation Time	16.426s	4.587s	4.072s
Vector / Matrix	Wideband DOA Estimation Methods		
	Extension 1 (37)	Extension 2 (40)	Extension 3 (44)
$\widetilde{\mathbf{r}}^{\circ}_{\mathbf{g}}$ / $\widetilde{\mathbf{r}}^{\circ}_{\mathbf{g}}$ / $\widetilde{\mathbf{r}}_{\mathbf{g}}$	54030	54030	54015
$\widetilde{\mathbf{z}}$ / $\check{\mathbf{z}}^{\circ}_{\mathbf{c}}$ /$\widetilde{\mathbf{z}}_{\mathbf{s}}$	1500	330	315
$\widetilde{\mathbf{B}}^{\circ}_{\mathbf{g}}$ / $\check{\mathbf{B}}^{\circ}_{\mathbf{cg}}$ / $\widetilde{\mathbf{B}}_{\mathbf{sg}}$	81045000	17829900	17014725
Computation Time	2146.594s	273.104s	255.137s

remain the same as the previous simulation examples. We set d_f to be 1.33. Then, for $Q = 15$ frequency bins, the first 8 frequency bins with $l = 17, 18, \cdots, 24$ satisfy $d \leq \lambda_l/2$ while the other 7 bins of $l = 25, 26, \cdots, 31$ satisfy $d > \lambda_l/2$. We use wideband extension 3 based on the modified low-complexity method (44) in our simulation. The results are shown in Fig. 6, where we can observe that all the 15 sources have been distinguished successfully.

To compare the estimation accuracy for different values of d_f with respect to a varied input SNR, the RMSE results of $d_f = 1$, $d_f = 1.33$ and $d_f = 1.6$ are shown in Fig. 7, where each point is based on an average of the results obtained by 500 simulation runs. Clearly, a relatively larger unit spacing d, corresponding to a larger d_f, yields more accurate results.

However, there is a limit to which an increase of d_f will lead to an improved performance. To show this, we fix the input SNR to 0 dB and the RMSE results versus d_f are shown in Fig. 8. In this example, since the frequency range is from 0.5π to π, we have $\lambda_{\max} = 2\lambda_{\min}$. Then $d = \lambda_{\max}/2$ corresponds to $d_f = 2$. So, we can expect $d_f = 2$ should still give a good performance, as verified in Fig. 8. Note that there are two factors guiding the best value for d or d_f. Increasing d, the aperture size is increased and so is resolution; on the other hand, an increase of d beyond the value of $\lambda_{\max}/2$ will cause aliasing problems for all frequencies and make the whole DOA estimation problem more difficult to solve. When d keeps increasing until some value beyond which, the gain due to a larger aperture size will be offset by the loss due to the increased difficulty. Therefore, we expect the performance becomes better with the initial increase of d, but gets worse when d is increased beyond some value. As shown in Fig. 8, for about $1.6 < d_f < 2.6$, the performance is quite flat, but $d_f = 2$ seems to be the middle point of this flat region, indicating that $d = \lambda_{\max}/2$ can be a reasonable choice in practice.

VI. EXPERIMENT RESULTS

To test the performance of the proposed algorithms in a real scenario, a co-prime microphone array system with $M = 2$ and $N = 5$ is set up for our experiment and there are $2M+N-1 = 8$ microphones in total. The received acoustic signals, after amplification, are then sampled through a data acquisition card (ADLINK's DAQ-2205) and stored in a computer. A picture of the system is shown in Figure 9. The sampling frequency f_s is set to be 20 kHz, and the frequency band of interest is from 5 kHz to 10 kHz giving a minimum wavelength of $\lambda_{\min} = 3.4$ cm at a speed of 340 m/s. Then, the equivalent unit spacing $d = \lambda_{\min}/2 = 1.7$ cm, and the positions of the two sub-array elements are given by

$$\begin{aligned} S_1 &= \{0, 3.4, 6.8, 10.2, 13.6\}\,\text{cm}\,, \\ S_2 &= \{0, 8.5, 17, 25.5\}\,\text{cm}\,. \end{aligned} \tag{45}$$

In this experiment, there are 10 uncorrelated acoustic source signals distributed from around -40° to 50° with an approximate step size of 10°. We apply the method in (44) to the collected data to obtain the DOA estimation results. The number of signal samples in the time domain for each microphone channel is 128000, and DFT of $L = 64$ points is applied. A search grid of $K_g = 3601$ incident angles is

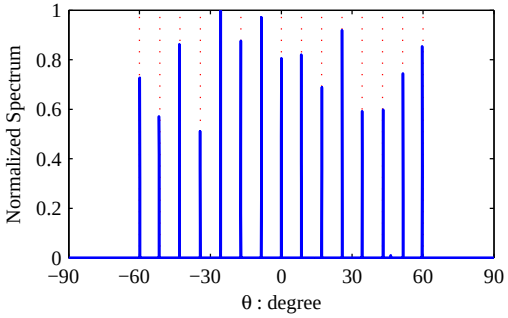

(a) Estimation results of existing method for single frequency.

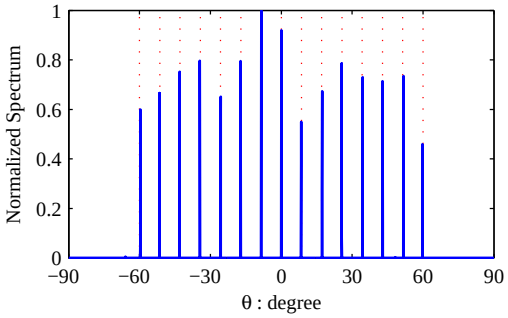

(b) Estimation results of proposed low complexity method for single frequency.

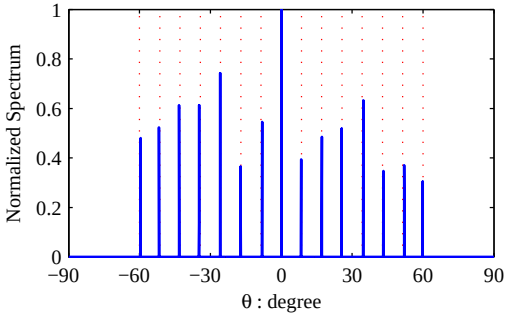

(c) Estimation results of modified low complexity method for single frequency.

Fig. 2. Estimation results obtained by the three narrowband methods. The dotted lines represent the actual incident angles of the impinging signals, while the solid lines represent the estimation results.

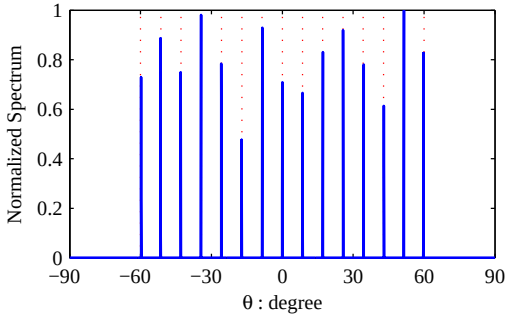

(a) DOA estimation results of wideband extension based on existing method.

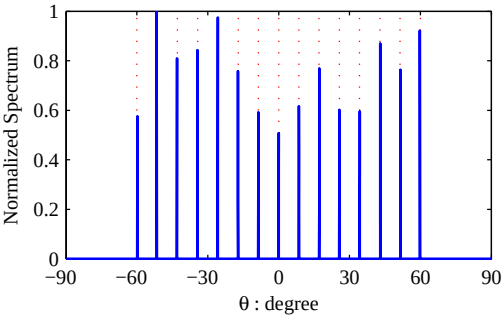

(b) DOA estimation results of wideband extension based on proposed low complexity method.

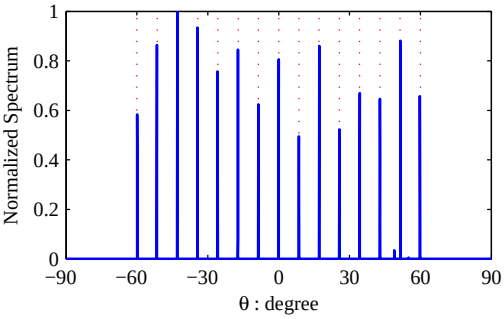

(c) DOA estimation results of wideband extension based on modified low complexity method.

Fig. 3. DOA estimation results obtained by the three wideband extensions.

formed within the full angle range with a step size of $0.05°$. The normalized frequency range of impinging signals covers the frequency bin set $\Phi_l = \{17, 18, \cdots, 31\}$ with $Q = 15$. These parameters are the same as the setting in Section V, and the results are shown in Fig. 10. It is evident that all the 10 sources have been distinguished successfully by the proposed method.

VII. Conclusion

A class of low-complexity compressive sensing based DOA estimation methods for wideband co-prime arrays have been proposed. We first derived a class of low-complexity narrowband DOA estimation methods, where a virtual array at each frequency bin with a much larger aperture is formed. Then redundant entries are combined in both auto-correlation and cross-correlation matrices to obtain more accurate approximations to the required correlation values. A further reduction in the computational complexity is achieved by removing noise power estimation from the formulation. By simultaneously exploiting the information at different frequency bins for the wideband case, a group-sparsity based optimisation problem is formulated which is amenable to application of existing convex optimisation toolboxes. This group-sparsity based method is further applied to co-prime arrays with a much larger unit spacing for better performances. It has been shown by simulations that our proposed methods in narrowband case have almost the same estimation performance, but with significantly lower computational complexity than the existing method. All these methods work effectively in the wideband case over a wide input SNR range, and achieve a much better estimation result than using one frequency only.

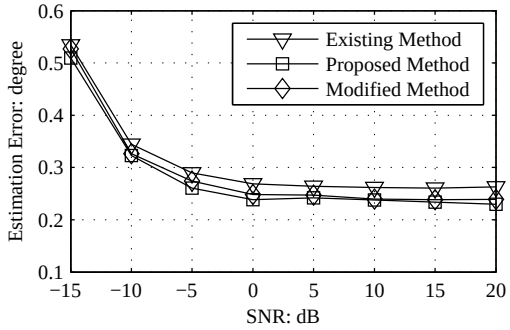

(a) RMSEs of different methods for single frequency.

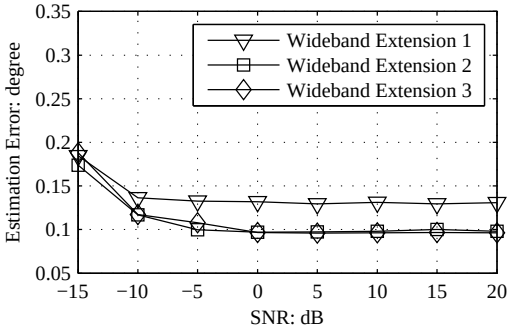

(b) RMSEs of different wideband extensions.

Fig. 4. RMSEs of different DOA estimations for single frequency and their wideband extensions versus input SNR.

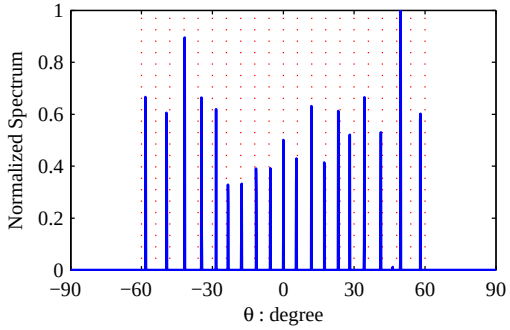

(a) Narrowband DOA estimation results.

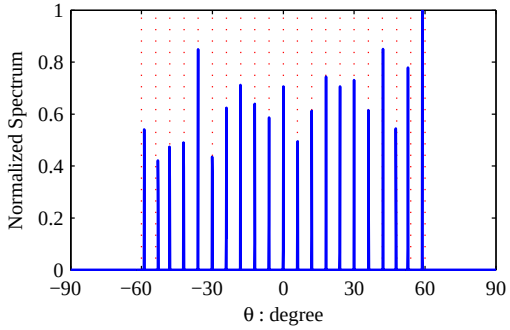

(b) Wideband DOA estimation results.

Fig. 5. DOA estimation results obtained by the modified low complexity narrowband method and its wideband extension.

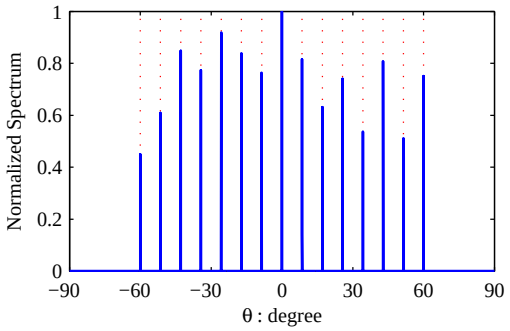

Fig. 6. DOA estimation results obtained by group sparsity based wideband method with $d_f = 1.33$.

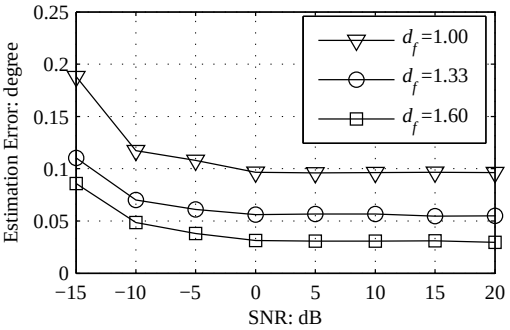

Fig. 7. RMSEs with different d_f versus input SNR.

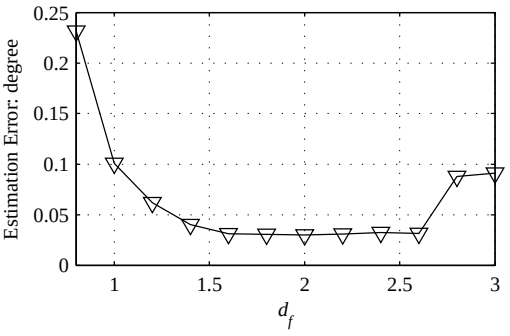

Fig. 8. RMSEs versus d_f.

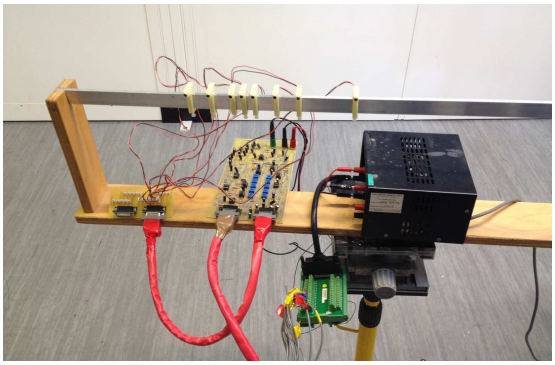

Fig. 9. The co-prime microphone array system for data collection.

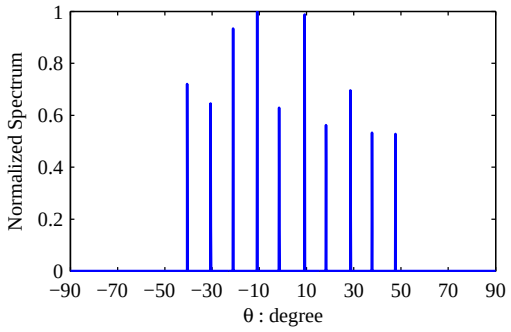

Fig. 10. Estimation results for collected acoustic data.

REFERENCES

[1] Q. Shen, W. Liu, W. Cui, S. L. Wu, Y. D. Zhang, and M. Amin, "Group sparsity based wideband DOA estimation for co-prime arrays," in *Proc. IEEE China Summit and International Conference on Signal and Information Processing*, Xi'an, China, Jul. 2014.

[2] Q. Shen, W. Liu, W. Cui, and S. L. Wu, "Low-complexity compressive sensing based DOA estimation for co-prime arrays," in *Proc. International Conference on Digital Signal Processing*, Hong Kong, China, Aug. 2014.

[3] M. S. Brandstein and D. Ward, Eds., *Microphone Arrays: Signal Processing Techniques and Applications*. Berlin: Springer, 2001.

[4] H. L. Van Trees, *Optimum Array Processing, Part IV of Detection, Estimation, and Modulation Theory*. New York: Wiley, 2002.

[5] W. Liu and S. Weiss, *Wideband Beamforming: Concepts and Techniques*. Chichester, UK: John Wiley & Sons, 2010.

[6] A. Moffet, "Minimum-redundancy linear arrays," *IEEE Trans. Antennas Propag.*, vol. 16, no. 2, pp. 172–175, Mar. 1968.

[7] R. T. Hoctor and S. A. Kassam, "The unifying role of the coarray in aperture synthesis for coherent and incoherent imaging," *Proc. IEEE*, vol. 78, no. 4, pp. 735–752, Apr. 1990.

[8] M. B. Hawes and W. Liu, "Location optimisation of robust sparse antenna arrays with physical size constraint," *IEEE Antennas and Wireless Propagation Letters*, vol. 11, pp. 1303–1306, November 2012.

[9] M. Crocco and A. Trucco, "Stochastic and analytic optimization of sparse aperiodic arrays and broadband beamformers with robust superdirective patterns," *IEEE Transactions on Audio, Speech, and Language Processing*, vol. 20, no. 9, pp. 2433–2447, November 2012.

[10] M. B. Hawes and W. Liu, "Compressive sensing based approach to the design of linear robust sparse antenna arrays with physical size constraint," *IET Microwaves, Antennas & Propagation*, vol. 8, no. 10, pp. 736–746, 2014.

[11] M. B. Hawes and W. Liu, "Sparse array design for wideband beamforming with reduced complexity in tapped delay-lines," *IEEE Trans. Audio, Speech and Language Processing*, vol. 22, pp. 1236–1247, August 2014.

[12] M. B. Hawes and W. Liu, "Design of Fixed Beamformers Based on Vector-Sensor Arrays" *International Journal of Antennas and Propagation*, vol. 2015, 2015 (DOI: 10.1155/2015/181937).

[13] P. P. Vaidyanathan and P. Pal, "Sparse sensing with co-prime samplers and arrays," *IEEE Trans. Signal Process.*, vol. 59, no. 2, pp. 573–586, Feb. 2011.

[14] P. Pal and P. P. Vaidyanathan, "Coprime sampling and the MUSIC algorithm," in *Proc. IEEE Digital Signal Processing Workshop and IEEE Signal Processing Education Workshop (DSP/SPE)*, Sedona, AZ, Jan. 2011, pp. 289–294.

[15] P. Pal and P. P. Vaidyanathan, "On application of LASSO for sparse support recovery with imperfect correlation awareness," in *Proc. Asilomar Conference on Signals, Systems and Computers (ASILOMAR)*, Pacific Grove, CA, Nov. 2012, pp. 958–962.

[16] Y. D. Zhang, M. G. Amin, and B. Himed, "Sparsity-based DOA estimation using co-prime arrays," in *Proc. IEEE International Conference on Acoustics, Speech and Signal Processing (ICASSP)*, Vancouver, Canada, May 2013, pp. 3967–3971.

[17] Y. D. Zhang, M. G. Amin, F. Ahmad, and B. Himed, "DOA estimation using a sparse uniform linear array with two CW signals of co-prime frequencies," in *Proc. IEEE International Workshop on Computational Advances in Multi-Sensor Adaptive Processing*, Saint Martin, Dec. 2013, pp. 404–407.

[18] T.-J. Shan, M. Wax, and T. Kailath, "On spatial smoothing for direction-of-arrival estimation of coherent signals," *IEEE Trans. Acoust., Speech, Signal Process.*, vol. 33, no. 4, pp. 806–811, Aug. 1985.

[19] W. Du and R. L. Kirlin, "Improved spatial smoothing techniques for DOA estimation of coherent signals," *IEEE Trans. Signal Process.*, vol. 39, no. 5, pp. 1208–1210, May 1991.

[20] G. Su and M. Morf, "The signal subspace approach for multiple wide-band emitter location," *IEEE Trans. Acoust., Speech, Signal Process.*, vol. 31, no. 6, pp. 1502–1522, Dec. 1983.

[21] H. Wang and M. Kaveh, "Coherent signal-subspace processing for the detection and estimation of angles of arrival of multiple wide-band sources," *IEEE Trans. Acoust., Speech, Signal Process.*, vol. 33, no. 4, pp. 823–831, Aug. 1985.

[22] Y.-S. Yoon, L. M. Kaplan, and J. H. McClellan, "TOPS: new DOA estimator for wideband signals," *IEEE Trans. Signal Process.*, vol. 54, no. 6, pp. 1977–1989, Jun. 2006.

[23] J.-Y. Lee, R. E. Hudson, and K. Yao, "Acoustic DOA estimation: An approximate maximum likelihood approach," *IEEE Systems Journal*, vol. 8, no. 1, pp. 131–141, Mar. 2014.

[24] Z.-M. Liu, Z.-T. Huang, and Y.-Y. Zhou, "Direction-of-arrival estimation of wideband signals via covariance matrix sparse representation," *IEEE Trans. Signal Process.*, vol. 59, no. 9, pp. 4256–4270, Sep. 2011.

[25] Z.-M. Liu, Z.-T. Huang, and Y.-Y. Zhou, "Sparsity-inducing direction finding for narrowband and wideband signals based on array covariance vectors," *IEEE Trans. Wireless Commun.*, vol. 12, no. 8, pp. 3896–3906, Aug. 2013.

[26] J.-A. Luo, X.-P. Zhang, and Z. Wang, "A new subband information fusion method for wideband DOA estimation using sparse signal representation," in *Proc. IEEE International Conference on Acoustics, Speech and Signal Processing (ICASSP)*, Vancouver, Canada, May 2013, pp. 4016–4020.

[27] S. Qin, Y. D. Zhang, and M. G. Amin, "Generalized coprime array configurations," in *Proc. IEEE Sensor Array and Multichannel Signal Processing Workshop*, A Coruna, Spain, Jun. 2014, pp. 529–532.

[28] M. Grant and S. Boyd. (2013, Dec.) CVX: Matlab software for disciplined convex programming, version 2.0 beta, build 1023. [Online]. Available: http://cvxr.com/cvx

[29] M. Grant and S. Boyd, "Graph implementations for nonsmooth convex programs," in *Recent Advances in Learning and Control*, ser. Lecture Notes in Control and Information Sciences, V. Blondel, S. Boyd, and H. Kimura, Eds. Springer-Verlag, 2008, pp. 95–110, http://stanford.edu/~boyd/graph_dcp.html.

Qing Shen was born in Jiangxi, China, in May 1988. He received his Bachelor's degree in Information Engineering from Beijing Institute of Technology, Beijing, China, in 2009. He is currently working towards his Ph.D. degree in the School of Information and Electronics, Beijing Institute of Technology, Beijing, China. He is also a visiting researcher in the Department of Electronic and Electrical Engineering, University of Sheffield, Sheffield, UK. His research interests include Radar and array signal processing.

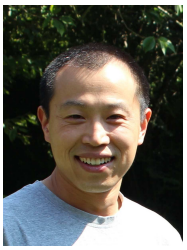

Wei Liu received his B.Sc. in 1996 and L.L.B. in 1997, both from Peking University, China, M.Phil. from University of Hong Kong, in 2001, and Ph.D. in 2003 from the School of Electronics and Computer Science, University of Southampton, UK. He later worked as a postdoc at Imperial College London. Since September 2005, he has been with the Department of Electronic and Electrical Engineering, University of Sheffield, UK, first as a lecturer, and then a senior lecturer. His research interests are in sensor array signal processing, blind signal processing, multirate signal processing and their various applications. He has now published about 160 journal and conference papers, three book chapters, and a research monograph about wideband beamforming ("Wideband Beamforming: Concepts and Techniques", John Wiley & Sons, March 2010, webpage: www.zepler.net/∼w.liu). He is a senior member of IEEE and currently an associate editor for IEEE Trans. Signal Processing.

Wei Cui received the B.S. degree in physics and Ph.D. degrees in electronics engineering from Beijing Institute of Technology, Beijing, China, in 1998 and 2003, respectively. From 2003 to 2005, he worked as a post-doctor in the school of information and electronics, Beijing Institute of Technology, where his research mainly concentrated on signal processing and its applications. He is currently a professor and Ph. D. supervisor in Beijing Institute of Technology, and his research interests include target detection and localization, theory and application of signal processing.

Siliang Wu received his Ph.D. degree in Electrical Engineering from Harbin Institute of Technology in 1995. He then worked as a post-doctor, and is now a professor in Beijing Institute of Technology. His current research interests include statistical signal processing, sensor array and multichannel signal processing, adaptive signal processing and their applications in radar, aerospace TT&C and satellite navigation. He has authored and co-authored more than 210 journal papers and holds 52 patents. He received one first-class prize of the National Award for TechnologicalInvention, and the Ho Leung Ho Lee Foundation Prize in 2014. He is also the recipient of the National May 1 LaborMedal and the National Model Teacher.

Yimin D. Zhang (SM'01) received his Ph.D. degree from the University of Tsukuba, Tsukuba, Japan, in 1988. He joined the faculty of the Department of Radio Engineering, Southeast University, Nanjing, China, in 1988. He served as a Director and Technical Manager at the Oriental Science Laboratory, Yokohama, Japan, from 1989 to 1995, and a Senior Technical Manager at the Communication Laboratory Japan, Kawasaki, Japan, from 1995 to 1997. He was a Visiting Researcher at the ATR Adaptive Communications Research Laboratories, Kyoto, Japan, from 1997 to 1998. Since 1998, he has been with the Villanova University, Villanova, PA, where he is currently a Research Professor with the Center for Advanced Communications, and is the Director of the Wireless Communications and Positioning Laboratory and the Director of the Radio Frequency Identification (RFID) Laboratory. His general research interests lie in the areas of statistical signal and array processing applied for radar, communications, and navigation, including compressive sensing, convex optimization, time-frequency analysis, MIMO system, radar imaging, target localization and tracking, wireless networks, and jammer suppression. He has published more than 250 journal articles and peer-reviewed conference papers and 11 book chapters.

Dr. Zhang serves on the Editorial Board of the Signal Processing journal. He was an Associate Editor for the IEEE TRANSACTIONS ON SIGNAL PROCESSING during 20102014, an Associate Editor for the IEEE SIGNAL PROCESSING LETTERS during 20062010, and an Associate Editor for the Journal of the Franklin Institute during 20072013. He is a member of the IEEE Signal Processing Societys Sensor Array and Multichannel Technical Committee.

Moeness G. Amin is the Director of the Center for Advanced Communications, Villanova University, Pennsylvania, USA. He is a Fellow of the Institute of Electrical and Electronics Engineers (IEEE); Fellow of the European Association for Signal Processing (EURASIP); Fellow of the International Society of Optical Engineering; and a Fellow of the Institute of Engineering and Technology (IET). Dr. Amin is the Recipient of the 2014 IEEE Signal Processing Society Technical Achievement Award; Recipient of the 2009 Individual Technical Achievement Award from EURASIP; Recipient of the 2015 IEEE Warren D White Award for Excellence in Radar Engineering; Recipient of the 2010 NATO Scientific Achievement Award; Recipient of the 2010 Chief of Naval Research Challenge Award; Recipient of 1997 Villanova University Outstanding Faculty Research Award; and the Recipient of the 1997 IEEE Philadelphia Section Award. He is a Recipient of the IEEE Third Millennium Medal, and was a Distinguished Lecturer of the IEEE Signal Processing Society, 2003-2004. Dr. Amin is currently the Chair of the Electrical Cluster of the Franklin Institute Committee on Science and the Arts. He has over 700 journal and conference publications in the theory and applications of signal processing. He co-authored 18 book chapters, and is the Editor of the two books "Through the Wall Radar Imaging" and "Compressive Sensing for Urban Radar," published by CRC Press in 2011 and 2014, respectively.